presence of a radical paramagnetic species (g = 2.00246, ΔH = 11.4 G). The reduced states $Zn{\cdot}2^+$ and $Zn{\cdot}2^0$, containing formally monovalent and zero-valent zinc, respectively, are better described as zinc(II) stabilized anion radicals. Clearly, the redox orbitals involved in the reduction process are ligand localized.

(h) Cadmium Complexes. As for its Zn^{2+} analogue, $Cd(\mathbf{1})_2^{2+}$ is unstable in DMF. The electrochemical study of $Cd(\mathbf{1})_2^{2+}$ and $Cd{\cdot}2^{2+}$ has thus been performed in CH_3CN and CH_2Cl_2. In CH_3CN, free Cd^{2+}, $Cd(\mathbf{1})_2^{2+}$, and $Cd{\cdot}2^{2+}$ are reduced in a two-electron process at −0.285, −0.400, and −0.850 V, respectively.

In each case, the divalent cadmium species is reduced to cadmium amalgam. This is confirmed by electrolysis at fixed potentials of either $Cd(\mathbf{1})_2^{2+}$ or $Cd{\cdot}2^{2+}$: reduction is accompanied by complete demetalation.

In CH_2Cl_2 and on Pt, the electrochemical behavior of $Cd{\cdot}2^{2+}$ is, however, different. The corresponding CV (not shown) indicates that reduction occurs in two steps at −1.15 and −1.36 V. The monovalent and zero-valent complexes could not be built-up in solution. However, it is remarkable that the mono- and direduced cadmium catenates could be observed as transient species when the dissociation reaction is not favored by amalgam formation. Here again, this particular property mainly originates from the interlocking of the ligand since reduction of $Cd(\mathbf{1})_2^{2+}$ under the same conditions leads only to complete dissociation with no observable transient species. At the present stage, it is difficult to know whether the formally cadmium(I) catenate corresponds to a real cadmium(I) complex, analogous to other recently described cage complexes,[74] or to a cadmium(II) stabilized radical anion.

Conclusions

The novel topological properties of the catenand **2** and the concomitant particular entwined shape of its complexes, the catenates, lead to new and surprising effects. A number of catenates, $M{\cdot}2^{n+}$ (M is the cationic species: Cu^{I}, Cu^{II}, Ag^{I}, Co^{II}, Ni^{II}, Zn^{II}, Cd^{II}, and Li^{I}), have been prepared and fully characterized by the usual physical methods. From a preparative viewpoint, several catenates appear to be noticeably more stable than their open-chain analogues with **1**, although the steric and electronic properties of $M{\cdot}2^{n+}$ and $M(\mathbf{1})_2^{n+}$ should be identical. The interlocked nature of **2** is responsible for this enhanced stability, allowing for the preparation of $Zn{\cdot}2^{2+}$, $Cd{\cdot}2^{2+}$, $Li{\cdot}2^{+}$, and $Ni{\cdot}2^{2+}$, whose analogous complexes with **1** could not be isolated in the solid state. ^{1}H NMR spectroscopy clearly shows that, for all the catenates studied, the geometry of the complex is roughly the same: the two dpp subunits are entwined and coordination of the metal occurs via the four nitrogen atoms of the ligand. The pentaoxyethylene fragments have not been found to interact with the complexed species, even in the case of $Li{\cdot}2^{+}$.

The most striking property of the catenand is its ability to stabilize low oxidation states of several transition metals. For instance, the existence range of the monovalent copper(I) catenate $Cu{\cdot}2^{+}$ lies around 2.2 V, both the oxidation and reduction products being still stable in solution. Other examples include $Zn{\cdot}2^{+}$, which can easily be made and studied in solution, and silver(I), which like $Cu{\cdot}2^{+}$ shows an unusually broad redox existence range (−0.7 to ligand oxidation starting around 1.5 V versus SCE). Monovalent cobalt, iron, and nickel catenates, $Co{\cdot}2^{+}$, $Fe{\cdot}2^{+}$, and $Ni{\cdot}2^{+}$, are also highly accessible by reduction, the nickel(I) complex being in addition kinetically inert toward its reoxidation by molecular oxygen. In most cases, comparison of the catenates with their acyclic analogues containing **1** shows a strong contribution of the topological factor of **2** to the ability to stabilize low oxidation states. The enhancement of stability of low oxidation state complexes of catenates as compared to their $M(\mathbf{1})_2^{n+}$ analogues has a profound effect on their kinetic properties. Whereas reduction potential values of $M{\cdot}2^{n+}$ and $M(\mathbf{1})_2^{n+}$ are in several instances very close, the kinetic stability of the reduced catenate with respect to *dissociation* or *reoxidation* is always noticeably more pronounced than that of the corresponding open-chain complex.

Acknowledgment. We thank the CNRS for financial support. Fruitful discussions with Professor P. Federlin and Dr. J. P. Kintzinger are also gratefully acknowledged. We also thank Dr. J. J. Andrē and M. Bernard for EPR spectra.

Registry No. **1**, 89333-97-1; $Co(\mathbf{1})_2^{2+}$, 121704-89-0; $Co(\mathbf{1})_2^{+}$, 121704-96-9; $Co(\mathbf{1})_2$, 121704-97-0; $Ni(\mathbf{1})_2^{2+}$, 98987-66-7; $Ni(\mathbf{1})_2^{+}$, 98987-65-6; $Ni(\mathbf{1})_2$, 121705-00-8; $Cu(\mathbf{1})_2^{2+}$, 121705-02-0; $Cu(\mathbf{1})_2^{+}$, 95246-98-3; $Cu(\mathbf{1})_2$, 121705-03-1; $Cu(\mathbf{1})_2^{-}$, 121705-04-2; $Zn(\mathbf{1})_2^{2+}$, 121730-26-5; $Zn(\mathbf{1})_2^{+}$, 121705-07-5; $Zn(\mathbf{1})_2$, 121705-08-6; $Ag(\mathbf{1})_2^{+}$, 121704-84-5; $Ag(\mathbf{1})_2$, 121705-11-1; $Cd(\mathbf{1})_2^{2+}$, 121704-91-4; $Cd(\mathbf{1})_2$, 121705-13-3; $Li{\cdot}2^{+}$, 121704-88-9; **Li·2**, 121704-92-5; $Li{\cdot}2^{-}$, 121704-93-6; $Fe{\cdot}2^{2+}$, 121704-94-7; $Fe{\cdot}2^{+}$, 121730-27-6; **Fe·2**, 121704-95-8; $Co{\cdot}2^{2+}$, 121704-90-3; $Co{\cdot}2^{+}$, 121704-98-1; **Co·2**, 121704-99-2; $Ni{\cdot}2^{2+}$, 99919-65-0; $Ni{\cdot}2^{+}$, 99919-56-9; **Ni·2**, 121705-01-9; $Cu{\cdot}2^{2+}$, 121704-83-4; $Cu{\cdot}2^{+}$, 88503-31-5; **Cu·2**, 121705-05-3; $Cu{\cdot}2^{-}$, 121705-06-4; $Zn{\cdot}2^{2+}$, 121704-86-7; $Zn{\cdot}2^{+}$, 121705-09-7; **Zn·2**, 121705-10-0; $Ag{\cdot}2^{+}$, 121704-85-6; **Ag·2**, 121705-12-2; $Cd{\cdot}2^{2+}$, 121704-87-8; $Cd{\cdot}2^{+}$, 121705-14-4; **Cd·2**, 121705-15-5; **2**, 90030-13-0; $H{\cdot}2^{+}$, 108703-53-3.

(74) Lardinois, P.; Rebena, I.; Hickel, B. *New J. Chem.* **1988**, *12*, 21.
(75) Gutman, V.; Schmid, R. *Monatsh. Chem.* **1969**, *100*, 2113.

Detection of Alkylperoxo and Ferryl, $(Fe^{IV}{=}O)^{2+}$, Intermediates during the Reaction of *tert*-Butyl Hydroperoxide with Iron Porphyrins in Toluene Solution

Ramesh D. Arasasingham, Charles R. Cornman, and Alan L. Balch*

Contribution from the Department of Chemistry, University of California, Davis, California 95616. *Received December 12, 1988*

Abstract: PFe^{II} and $PFe^{III}OH$ (P is a porphyrin dianion) catalyze the decomposition of *tert*-butyl hydroperoxide in toluene solution without appreciable attack on the porphyrin ligand. ^{1}H NMR spectroscopic studies at low temperature (−70 °C) give evidence for the formation of a high-spin, five-coordinate intermediate, $PFe^{III}OOC(CH_3)_3$. On warming this decomposes to $PFe^{III}OH$ (P = tetramesitylporphyrin, TMP) or $PFe^{III}OFe^{III}P$ (P = tetra-*p*-tolylporphyrin, TTP) with the formation of $(TMP)Fe^{IV}{=}O$ as an observed intermediate in the first case. Treatment of $PFe^{III}OOC(CH_3)_3$ at −70 °C with *N*-methylimidazole (MeIm) yields the intermediate $(MeIm)PFe^{IV}{=}O$. Organic products formed from this reaction are *tert*-butyl alcohol, di-*tert*-butyl peroxide, benzaldehyde, acetone, and benzyl-*tert*-butyl peroxide, which arise largely from a radical chain process initiated by the iron porphyrin but continuing without its intervention.

The peroxidase, catalase, and cytochrome P-450 enzymes utilize alkyl hydroperoxides to generate high-valent oxoiron porphyrins.[1-3] Extensive studies on the peroxidase-catalyzed oxidations have established that the enzyme reacts with hydroperoxides to form

0002-7863/89/1511-7800$01.50/0

two distinct high-valent intermediates known as compounds I and II. Compound I is two oxidizing equivalents above the iron(III) state and is formulated as a ferrylporphyrin π-cation radical, $[(P^{\bullet})Fe^{IV}{=}O]^{+}$. The one-electron reduction of compound I yields compound II, which is described as a neutral ferryl complex, $[(P)Fe^{IV}{=}O]$. The reaction sequence is summarized as follows, where Enz is the active enzyme and AH_2 is a reducing substrate.

$$\text{Enz} + \text{ROOH} \rightarrow \text{compound I} + \text{ROH} \quad (1)$$

$$\text{compound I} + AH_2 \rightarrow \text{compound II} + AH^{\bullet} \quad (2)$$

$$\text{compound II} + AH_2 \rightarrow \text{Enz} + AH^{\bullet} \quad (3)$$

$$AH^{\bullet} \rightarrow \text{nonradical products} \quad (4)$$

Catalase and cytochrome P-450 are related to peroxidase in that they react with alkyl hydroperoxides to form a high oxidation state that is probably similar to that of compound I.[2,3]

Studies on natural heme proteins and on model systems have suggested that one of the key steps in these processes is the cleavage of the O–O bond of iron-coordinated hydroperoxides to generate the highly oxidized states.[4-15] Although iron alkyl hydroperoxide complexes have been postulated as intermediates in these processes, they have not been spectroscopically observed.

In order to explore the chemical behavior of iron-coordinated alkyl hydroperoxides and to provide structural models, we have undertaken a study of the interactions between iron porphyrins and *tert*-butyl hydroperoxide. This work complements our earlier studies involving the detection of alkylperoxo complexes of iron porphyrins produced via the insertion of dioxygen across iron(III)–carbon bonds[15-17] (eq 5). (Abbreviations used are the

$$PFe^{III}CHR_2 \xrightarrow{O_2} PFe^{III}OOCHR_2 \quad (5)$$

following: P, a porphyrin dianion; (P$^{\bullet}$), a porphyrin radical monoanion; TTP, dianion of porphyrin TMP, dianion of tetramesitylporphyrin; *N*-MeIm, *N*-methylimidazole.) In that work we showed that $PFe^{III}OOCH_2CH_3$ has a ^{1}H NMR spectrum typical of a high-spin, five-coordinate iron porphyrin and that it decomposed on warming to $PFe^{III}OH$ and acetaldehyde without forming spectroscopically detectable intermediates. For this reaction, likely paths include homolysis of the O–O bond followed by rapid oxidation of the radical (path a, eq 6), a concerted path with O–O

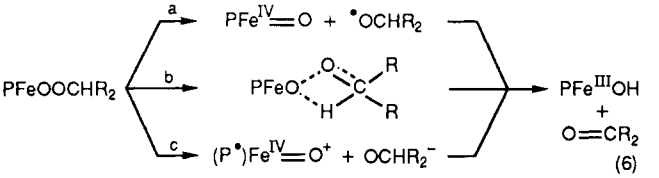

(6)

and C–H bond breaking occurring as the O–H bond is formed (path b, eq 6), or heterolysis of the O–O bond to give an oxidized ferryl complex (at the peroxidase compound I level of oxidation) and an alkoxide ion, which rapidly loses hydride to the oxidized ferryl complex (path c, eq 6). Neither $PFe^{IV}{=}O$[18,19] or $(P^{\bullet})Fe^{IV}{=}O$[19,20] (both of which have been detected by ^{1}H NMR studies on (TMP)Fe systems) was observed during decomposition of $PFe^{III}OOCH_2CH_3$.[15-17] However, we expected that if a suitable derivative lacking α-hydrogen atoms (e.g., $PFeOOC(CH_3)_3$) were available, then the intermediates might become observable. Unfortunately, we have not been able to use the dioxygen insertion route to prepare $PFeOOCR_3$ since numerous attempts to prepare $PFe^{III}C(CH_3)_3$ or $PFe^{III}CF_3$ have been unsuccessful. Hence, we have turned to examine the direct reaction of *tert*-butyl hydroperoxide with iron porphyrins in a system where the porphyrin ligand is not itself destroyed.

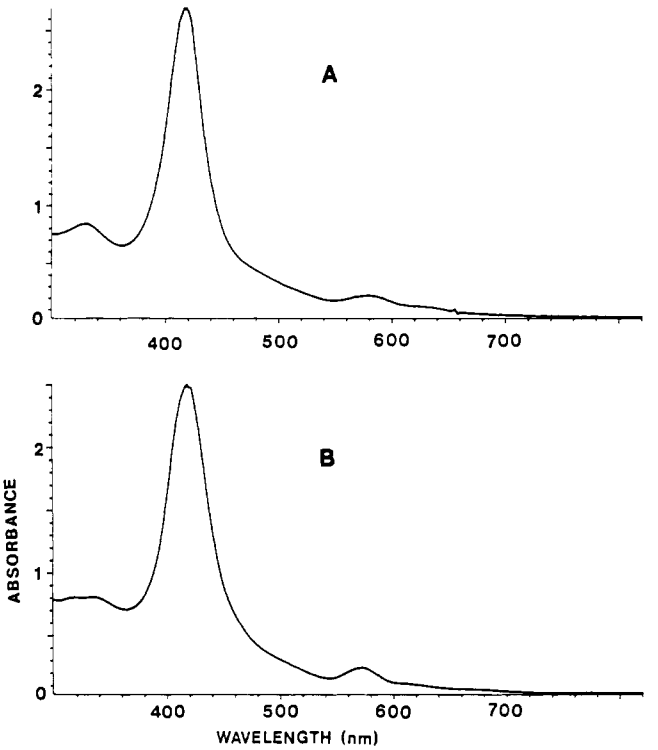

Figure 1. Electronic absorption spectrum of a toluene solution of $(TMP)Fe^{III}OH$: (A) before and (B) after reaction with 10 equiv of *tert*-butyl hydroperoxide.

Results

tert-Butyl hydroperoxide reacts with $(TTP)Fe^{II}$ or $(TMP)Fe^{III}OH$ in toluene solution with the loss of the hydroperoxide but no significant destruction of the porphyrin. Figure 1 shows the optical spectra of $(TMP)Fe^{III}OH$ before (trace A) and after (trace B) reaction with *tert*-butyl hydroperoxide. ^{1}H NMR analysis of

(1) (a) Saunders, B. C.; Homes-Siedel, A. G.; Stark, B. P. *Peroxidases*; Butterworths: London, 1964. (b) Hewson, W. D.; Hager, L. D. *Porphyrins* **1979**, *7*, 295. (c) Saunders, B. C. In *Inorganic Biochemistry*; Eichorn, G. I., Ed.; Elsevier: Amsterdam, The Netherlands, 1973; Vol. 2, p 988. (d) Dunford, H. B. *Adv. Inorg. Biochem.* **1982**, *4*, 41. Dunford, H. B.; Stillman, J. S. *Coord. Chem. Rev.* **1976**, *19*, 187.

(2) Schonbaum, G. R.; Chance, B. Catalase. In *The Enzymes*; Boyer, P., Ed.; Academic Press: New York, 1976; Vol. 13, p 363.

(3) Ortiz de Montellano, P. *Cytochrome P-450: Structure, Mechanism and Biochemistry*; Plenum Press: New York, 1986.

(4) White, R. E.; Coon, M. J. *Annu. Rev. Biochem.* **1980**, *49*, 315.

(5) Sligar, S. G.; Kennedy, K. A.; Pearson, D. C. *Proc. Natl. Acad. Sci. U.S.A.* **1980**, *77*, 1240.

(6) White, R. E.; Sligar, S. G.; Coon, M. J. *Biol. Chem.* **1980**, *255*, 11108.

(7) Traylor, T. G.; Lee, W. A.; Stynes, D. J. *J. Am. Chem. Soc.* **1984**, *106*, 755.

(8) Lee, W. A.; Bruice, T. C. *J. Am. Chem. Soc.* **1985**, *107*, 513.

(9) Mansuy, D.; Battioni, P.; Renaud, J. R. *J. Chem. Soc., Chem. Commun.* **1984**, 1255.

(10) Groves, J. T.; Watanabe, Y. *J. Am. Chem. Soc.* **1986**, *108*, 7834.

(11) Marnett, L. J.; Weller, P.; Battista, J. R. In *Cytochrome P-450: Structure, Mechanisms, and Biochemistry*; Ortiz de Montellano, P., Ed.; Plenum Press: New York, 1986; p 29.

(12) Bruice, T. C.; Zipplies, M. F.; Lee, W. *Proc. Natl. Acad. Sci. U.S.A.* **1986**, *83*, 4646.

(13) Traylor, T. G.; Xu, F. *J. Am. Chem. Soc.* **1987**, *109*, 6201.

(14) Lee, W. A.; Yuan, L.-C.; Bruice, T. C. *J. Am. Chem. Soc.* **1988**, *110*, 4277. Balasubramanian, P. N.; Lindsay Smith, J. R.; Davis, M. J.; Kaaret, T. W.; Bruice, T. C. *J. Am. Chem. Soc.* **1989**, *111*, 1477.

(15) Arasasingham, R. D.; Balch, A. L.; Latos-Grazynski, L. *J. Am. Chem. Soc.* **1987**, *109*, 5846.

(16) Arasasingham, R. D.; Balch, A. L.; Latos-Grazynski, L. In *Studies in Organic Chemistry*; Ando, W., Moro-oka, Y., Eds.; Elsevier: Amsterdam, The Netherlands, 1987; Vol. 33, p 417.

(17) Arasasingham, R. D.; Balch, A. L.; Cornman, C. R.; Latos-Grazynski, L. *J. Am. Chem. Soc.* **1989**, *111*, 4357.

(18) Balch, A. L.; Chan, Y. W.; Cheng, R. J.; La Mar, G. N.; Latos-Grazynski, L.; Renner, M. W. *J. Am. Chem. Soc.* **1984**, *106*, 7779.

(19) Balch, A. L.; Latos-Grazynski, L.; Renner, M. W. *J. Am. Chem. Soc.* **1985**, *107*, 2983.

(20) Groves, J. T.; Haushalter, R. C.; Nakamura, M.; Nemo, T. E.; Evans, B. J. *J. Am. Chem. Soc.* **1981**, *103*, 2884.

Table I. ^{1}H NMR Data for Relevant Iron Porphyrins in Toluene-d_8 Solution

compd	temp, °C	chemical shifts,[a] ppm				ref
			phenyl substituents			
		pyrrole	ortho	meta	para	
(TMP)FeOH	−70	116.4		14.9, 13.0	5.1	21
(TMP)FeO-*t*-Bu[a]	−70	122		20.3, 17.7		this work
(TTP)FeOO-*t*-Bu	−70	113	b	13.0, 11.6	6.1	this work
(TMP)FeOO-*t*-Bu	−70	114	b	15.3, 13.4	4.0	this work
(TMP)Fe^{IV}O	−70	8.4	3.3	6.4, 6.0	2.6	18
(*N*-MeIm)(TMP)Fe^{IV}O	−30	4.6	3.2, 1.6	7.4	2.7	18
(TMP$^•$)Fe^{IV}O	−70	−21	25, 28	62	10	19, 20

[a] Methyls of *t*-Bu at 46.5. [b] Not observed due to line broadening.

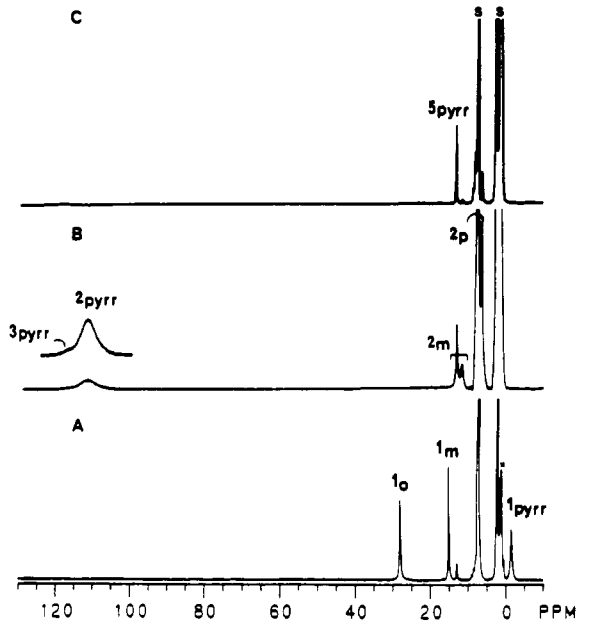

Figure 2. 360-MHz ^{1}H NMR spectra recording the reaction between (TTP)Fe^{II} and *t*-BuOOH in toluene-d_8 solution: (A) (TTP)Fe^{II} alone at −70 °C; (B) sample from A after the addition of *t*-BuOOH at −70 °C; (C) sample from B after warming to 25 °C and cooling to −70 °C. Peaks of (TTP)Fe^{II} are labeled **1**, those of (TTP)Fe^{III}OO-*t*-Bu are **2**, those of (TTP)Fe^{III}OH are **3**, and those of (TTP)Fe^{III}OFe^{III}(TTP) are **5**. Subscripts refer to the following assignments: pyrr, pyrrole; m, *m*-phenyl; o, *o*-phenyl; p, *p*-methyl.

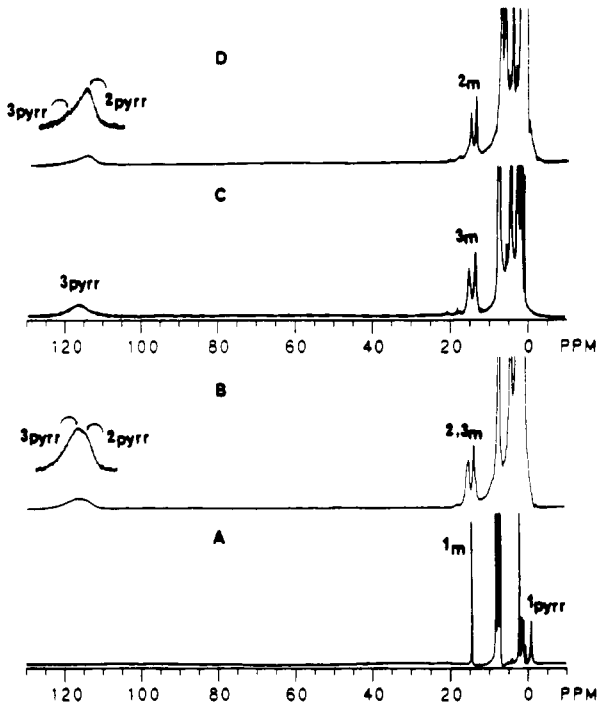

Figure 3. 360-MHz ^{1}H NMR spectra in toluene-d_8 at −70 °C: (A) (TMP)Fe^{II}; (B) (TMP)Fe^{II} and *t*-BuOOH; (C) (TMP)Fe^{III}OH; (D) (TMP)Fe^{III}OH + *t*-BuOOH after 25 h at −80 °C. Peaks are labeled as in Figure 1 except for the change in porphyrin.

the sample used to record trace B (before dilution) indicates that no *tert*-butyl hydroperoxide is present; *tert*-butyl alcohol and di-*tert*-butyl peroxide are readily detected, however. Notice that there is no significant loss of intensity in the porphyrin visible spectrum between traces A and B. ^{1}H NMR analysis shows that the iron porphyrin is present as a mixture of (TMP)Fe^{III}OH and (TMP)Fe^{III}OBu after reaction. Similar reactions with PFe^{II} and *tert*-butyl hydroperoxide in toluene show a rapid color change from the red of the Fe^{II} complex to the usual green/brown color of high-spin iron(III) porphyrins without bleaching. When the reaction is monitored at low temperature by ^{1}H NMR spectroscopy, it has been possible to detect and identify the iron porphyrin complexes that form during the processes. Relevant ^{1}H NMR spectral data both for previously observed components and for the newly observed hydroperoxide complexes are given in Table I.[18-21]

Formation of PFe^{III}OO-*t*-Bu. Figure 2 shows the ^{1}H NMR spectral changes that occur when a toluene-d_8 solution of (TTP)Fe^{II} is treated with excess *tert*-butyl hydroperoxide. Trace A shows the spectrum of (TTP)Fe^{II} at −70 °C. Trace B shows the spectrum of that sample after the addition of excess *tert*-butyl hydroperoxide at −70 °C. At this stage, (TTP)Fe^{II} has reacted, and two new species with similar resonance patterns are detected. These resonance patterns are indicative of high-spin ($S = {}^5/_2$), five-coordinate iron(III) species. On warming, both decay to give (TTP)Fe^{III}OFe^{III}(TTP) (**5**) as the principal product.[22] Notice that this behavior parallels that seen for the intermediates, (TTP)Fe^{III}OOCH$_2$CH$_3$ and (TTP)Fe^{III}OH, that are generated in the reaction between dioxygen and (TTP)Fe^{III}CH$_2$CH$_3$.[15-17] Trace C shows the spectrum of the sample after warming to 25 °C and then cooling to −70 °C. The intensities of the resonances of the high-spin species have decayed considerably, and these are replaced by the resonances of the μ-oxo dimer. On the basis of its chemical shift, the low-field pyrrole resonance in trace B can be identified as (TTP)Fe^{III}OH, which has been prepared independently through the reaction of hydroxide with (TTP)Fe^{III}Cl[21,23] and also by the thermal decomposition of (TTP)Fe^{III}O$_2$C$_2$H$_5$ generated through the reaction of dioxygen with (TTP)Fe^{III}C$_2$H$_5$.[15-17] It has been shown independently that (TTP)Fe^{III}OH readily undergoes dehydration to form the μ-oxo dimer.[23] The other high-spin intermediate is not (TTP)Fe^{III}O-*t*-Bu since, in particular, it lacks the appropriate *tert*-butyl resonance at 46.5 ppm.[24] Consequently, we identify this intermediate as (TTP)Fe^{III}OO-*t*-Bu.

Addition of *tert*-butyl hydroperoxide at −70 °C to a toluene-d_8 solution of the sterically hindered complex (TMP)Fe^{II} produces

(21) Cheng, R. J.; Latos-Grazynski, L.; Balch, A. L. *Inorg. Chem.* **1982**, *22*, 2412.

(22) For ^{1}H NMR characteristics, see: La Mar, G. N.; Eaton, G. R.; Holm, R. H.; Walker, F. A. *J. Am. Chem. Soc.* **1973**, *95*, 63.

(23) Fielding, L.; Eaton, G. R.; Eaton, S. S. *Inorg. Chem.* **1985**, *24*, 2309.

(24) Arafa, I. M.; Goff, H. M.; David, S. S.; March, B. P.; Que, L., Jr. *Inorg. Chem.* **1987**, *26*, 2779.

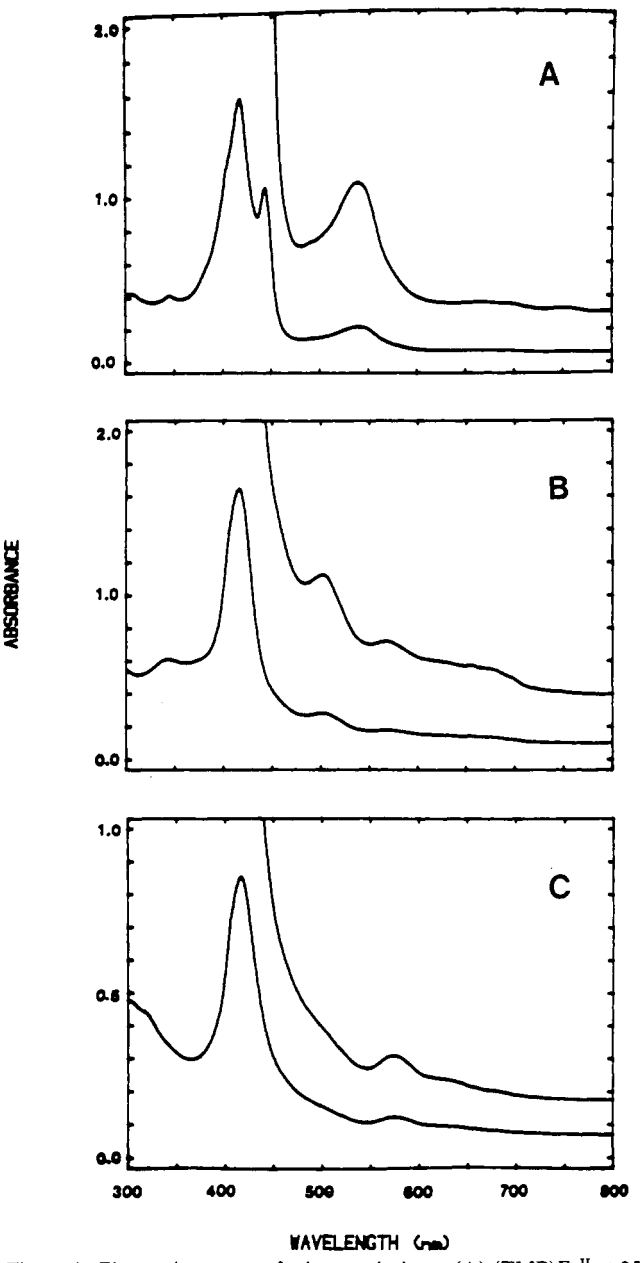

Figure 4. Electronic spectra of toluene solutions: (A) (TMP)Fe^{II} at 25 °C; (B) same sample of (TMP)Fe^{II} after adding *t*-BuOOH at −78 °C; (C) (TMP)Fe^{III}OH at −78 °C.

related changes. Traces A and B of Figure 3 compare the ^{1}H NMR spectra of a solution of (TMP)Fe^{II} before (trace A) and after (trace B) the addition of *tert*-butyl hydroperoxide. As before, the iron(II) species is entirely consumed, and resonances attributable to two new high-spin, five-coordinate iron(III) complexes have developed. On warming, resonances of one of these decay, while those of the other remain (vide infra). The resonances that remain correspond to the low-field pyrrole resonance seen in trace B of Figure 2 and are due to (TMP)Fe^{III}OH. This is thermally stable and does not undergo dehydration.[21] The ^{1}H NMR spectrum of pure (TMP)Fe^{III}OH is shown in trace C of Figure 3.

Incubation of *tert*-butyl hydroperoxide with (TMP)Fe^{III}OH for 24 h in toluene-d_8 solution at −80 °C produces the ^{1}H NMR spectrum shown in trace D of Figure 3. Notice that the resulting spectrum is similar to that shown in trace B but that the intensities of the resonances due to (TMP)Fe^{III}OH are lower in trace D. The second species present in the spectrum in trace D is again identified as (TMP)$Fe^{III}O_2$-*t*-Bu. In related experiments, treatment of (TMP)Fe^{III}OH with *tert*-butyl alcohol yields NMR resonances consistent with the formation of (TMP)Fe^{III}O-*t*-Bu.[24] Thus the

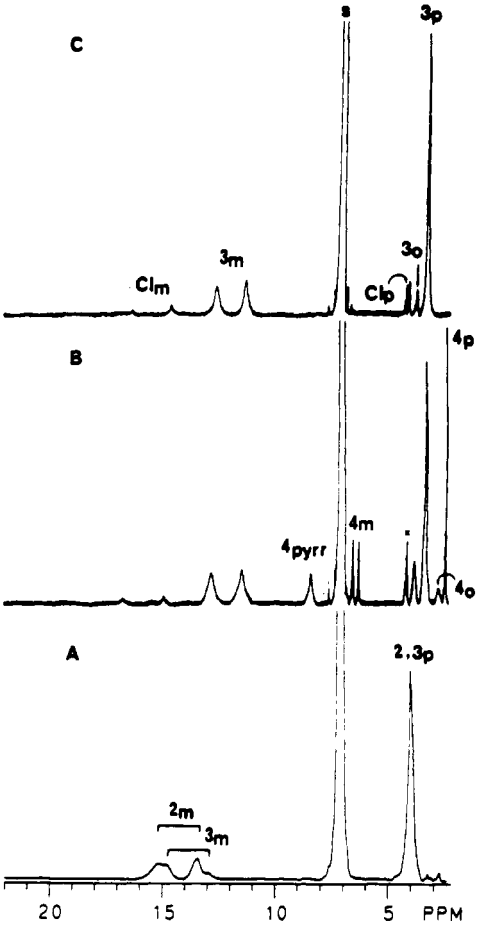

Figure 5. 360-MHz ^{1}H NMR of (TMP)Fe^{II} and *t*-BuOOH at −70 °C: (A) principle components (TMP)Fe^{III}OO-*t*-Bu and (TMP)Fe^{III}OH; (B) sample after warming to −10 °C; (C) sample after warming to 0 °C. Peaks are labeled in accord with Figure 1, with **4** denoting resonances from (TMP)Fe^{IV}=O.

exchange of one axial ligand for another is precedented.

Optical spectral changes consistent with the formation of these new species have also been observed. Trace A of Figure 4 shows the optical spectrum of (TMP)Fe^{II} in toluene at 23 °C. The spectrum shows only minor changes on cooling. Trace B shows the spectrum obtained from a mixture of (TMP)Fe^{II} and *tert*-butyl hydroperoxide at −78 °C. For comparison, the spectrum of (TMP)Fe^{III}OH in toluene at −78 °C is shown in trace C. Traces B and C are clearly different, and the differences are ascribed to the presence of the peroxy complex (TMP)Fe^{III}OO-*t*-Bu. Most characteristic of this species is a new absorption maximum at 500 nm.

Studies of the Reactivity of PFe^{III}OO-*t*-Bu. Warming solutions containing (TMP)$Fe^{III}O_2$-*t*-Bu produces unique ^{1}H NMR spectral changes that are not seen with (TMP)Fe^{III}OH alone, which is unchanged upon warming. Characteristic data are shown in Figure 5 where the initial sample was produced by the (TMP)-Fe^{II}/*t*-BuOOH reaction. Trace A shows a spectrum corresponding to that in trace B of Figure 3 in the 20–2 ppm region. Two sets of resonances in the 12–16 ppm region are due to the meta protons of (TMP)Fe^{III}OH and (TMP)$Fe^{III}O_2$-*t*-Bu. Trace B of Figure 5 shows the spectrum obtained after warming the sample to −10 °C. A new set of resonances has developed. These are due to (TMP)Fe^{IV}=O, which has previously been observed after warming (TMP)$Fe^{III}O_2Fe^{III}$(TMP).[18] The spectrum seen in trace B of Figure 5 can be compared to trace III of Figure 2 in ref 18 where an identical set of resonances is seen. In addition to resonances of (TMP)Fe^{IV}=O, a small amount of (TMP)Fe^{III}Cl has formed as a consequence of a small amount of chloride remaining from the reduction of (TMP)Fe^{III}Cl, which was used to form (TMP)Fe^{II}. The two resonances in the 11–14 ppm region are now symmetric in shape. Thus, all (TMP)$Fe^{III}O_2$-*t*-Bu has reacted,

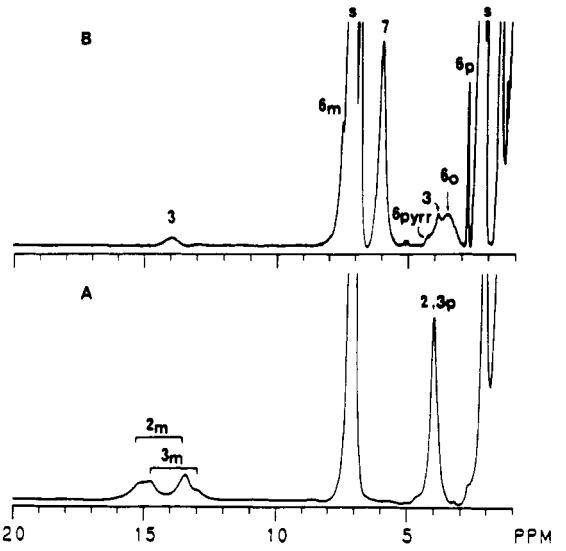

Figure 6. 360-MHz ^{1}H NMR spectra of toluene-d_8 solutions at −70 °C: (A) (TMP)Fe^{II} and *t*-BuOOH [principle components are (TMP)Fe^{III}OO-*t*-Bu and (TMP)Fe^{III}OH]; (B) that sample after the addition of excess *N*-methylimidazole. Peaks are labeled as in preceding figures, with **6** indicating resonances of (TMP)Fe^{IV}=O (*N*-MeIm), and **7**, *N*-methylimidazole.

but (TMP)Fe^{III}OH is still present. At this state of the reaction, recording the ^{1}H NMR spectrum in the 5–0 ppm region under conditions appropriate for observation of diamagnetic substances shows that no *tert*-butyl hydroperoxide remains. *tert*-Butyl alcohol and di-*tert*-butyl peroxide are present. Further warming to 0 °C results in the spectral changes seen in trace C of Figure 5. Resonances of (TMP)Fe^{IV}=O have disappeared, leaving (TMP)Fe^{III}OH and a trace of (TMP)Fe^{III}Cl. Virtually identical spectral changes are seen when a sample prepared from the (TMP)Fe^{III}OH/*t*-BuOOH reaction is warmed.

Figure 6 shows the effect of adding *N*-methylimidazole to a mixture of (TMP)Fe^{III}OH and (TMP)Fe^{III}O$_2$-*t*-Bu that was obtained from the (TMP)Fe^{II}/*tert*-butyl hydroperoxide reaction. Trace A shows the spectrum obtained before the addition of *N*-methylimidazole, while trace B shows the spectrum after the addition of excess *N*-methylimidazole. A set of new resonances is observed in the 0–10 ppm region. These are due to (*N*-MeIm)(TMP)Fe^{IV}=O. The reader should compare trace B of Figure 6 to trace II of Figure 7 in ref 18. The resonances due to (*N*-MeIm)(TMP)Fe^{IV}=O are unstable, and warming to 25 °C results in their decay. In addition, at −70 °C there is a single resonance at 14 ppm. This is due to the (TMP)Fe^{III}OH/*N*-methylimidazole system. Independent observations on solutions of (TMP)Fe^{III}OH in the presence of *N*-methylimidazole indicate that the usual meta doublet of (TMP)Fe^{III}OH collapses into a single resonance in these mixtures at −70 °C. The equilibria responsible for this are under further study.

Identification of Organic Products Resulting from *tert*-Butyl Hydroperoxide Decomposition. While the previous ^{1}H NMR studies have allowed the iron porphyrin species formed in the reaction with *tert*-butyl hydroperoxide to be observed, the fate of the *tert*-butyl hydroperoxide and involvement of the solvent, toluene, in the process need to be addressed. Consequently, the organic products have been monitored by both ^{1}H NMR spectroscopy and gas chromatography.

When (TMP)Fe^{II} is treated with a 10-fold excess of *tert*-butyl hydroperoxide at −70 °C in toluene under conditions similar to those used for the ^{1}H NMR observation and then warmed to room temperature, the hydroperoxide was consumed and the following products (mole percent) are formed: *tert*-butyl alcohol (87%), di-*tert*-butyl peroxide (7%), benzaldehyde (4%), and acetone (2%) along with trace quantities of benzyl-*tert*-butyl peroxide. When (TMP)Fe^{III}OH is treated with a 10-fold excess of *tert*-butyl hydroperoxide in toluene at 23 °C, the peroxide decomposes and the products are similar: *tert*-butyl alcohol (92%), di-*tert*-butyl peroxide (3%), benzaldehyde (3%), acetone (2%), and traces of benzyl-*tert*-butyl peroxide.

Discussion

The reactions that we believe yield (TMP)Fe^{III}OO-*t*-Bu are given below (eq 7–11). These are similar to those proposed by Espenson and Melton[25] for the formation of Co^{III}(dmgH)$_2$(OO-*t*-Bu)py from the reaction of *t*-BuOOH with Co^{II}(dmgH)$_2$py in benzene (dmgH = dimethylglyoxime monoanion). A corresponding stable hydroperoxide cobalt(III) complex has been obtained from cumyl hydroperoxide, crystallized, and structurally characterized by X-ray diffraction.[26]

$$PFe^{II} + t\text{-BuOOH} \rightarrow PFe^{III}OH + t\text{-BuO}^{\bullet} \quad (7)$$

$$t\text{-BuO}^{\bullet} + t\text{-BuOOH} \rightarrow t\text{-BuOH} + t\text{-BuOO}^{\bullet} \quad (8)$$

$$PFe^{II} + t\text{-BuOO}^{\bullet} \rightarrow PFe^{III}OO\text{-}t\text{-Bu} \quad (9)$$

$$\text{net: } \underset{\mathbf{1}}{2PFe^{II}} + 2\,t\text{-BuOOH} \rightarrow \underset{\mathbf{2}}{PFe^{III}OO\text{-}t\text{-Bu}} + \underset{\mathbf{3}}{PFe^{III}OH} + t\text{-BuOH} \quad (10)$$

$$\underset{\mathbf{3}}{PFe^{III}OH} + t\text{-BuOOH} \rightarrow \underset{\mathbf{2}}{PFe^{III}OO\text{-}t\text{-Bu}} + H_2O \quad (11)$$

Both **2** and **3** have been directly observed at low temperatures to result from the reaction of *tert*-butyl hydroperoxide and (TMP)Fe^{II}. Their ^{1}H NMR resonance patterns are consistent with their formulations as high-spin ($S = {}^5/_2$), five-coordinate iron(III) complexes.[21]

The organic product distribution that we observe suggests that *tert*-butyl hydroperoxide has been decomposed through a free-radical path[27-32] that is initiated by the iron porphyrins. Reaction 7, which generates *t*-BuOO$^{\bullet}$, serves to initiate the radical chain when iron(II) is present. The chain continues through reactions 8 and 12. Eventually all of the hydroperoxide is destroyed. The

$$2\,t\text{-BuOO}^{\bullet} \longrightarrow [t\text{-BuO}_4\text{Bu-}t]_{\text{cage}} \xrightarrow{\text{propagation}} 2\,t\text{-BuO}^{\bullet} + O_2 \quad (12a)$$

$$[t\text{-BuO}_4\text{Bu-}t]_{\text{cage}} \xrightarrow{\text{termination}} t\text{-BuO}_2\text{Bu-}t + O_2 \quad (12b)$$

formation of di-*tert*-butyl peroxide is evidence for the formation of *t*-BuOO$^{\bullet}$, since the alternative, combination of two *t*-BuO$^{\bullet}$, has been shown to be unimportant in solution.[27,28] Benzaldehyde is formed by attack upon solvent, and acetone is formed from *tert*-butoxy radicals. The product distribution is similar regardless of whether we initiate the *tert*-butyl hydroperoxide decomposition with PFe^{II} or PFe^{III}OH. The formation of **2** from PFeOH and *t*-BuOOH (reaction 11) is not sufficient to initiate the free-radical chain. Either there is reduction of some PFe^{III}OH to PFe^{II} or another reaction (e.g., reaction 13, vide infra) serves to initiate the chain.

With the sterically constrained porphyrin, (TMP)H$_2$, thermal decomposition of (TMP)FeOO-*t*-Bu (**2**) has been shown to produce a second detectable intermediate, identified as the ferryl complex (TMP)Fe^{IV}=O (**4**). We believe the formation of **4** results from the homolytic cleavage of the (TMP)Fe^{III}OO-*t*-Bu

(25) Espenson, J. H.; Melton, J. D. *Inorg. Chem.* **1983**, *22*, 2779.
(26) Giannotti, C.; Fontaine, C.; Chiaroni, A.; Riche, C. *J. Organomet. Chem.* **1976**, *113*, 75.
(27) Hiatt, R.; Traylor, T. G. *J. Am. Chem. Soc.* **1965**, *87*, 3766.
(28) Factor, A.; Russell, C. A.; Traylor, T. G. *J. Am. Chem. Soc.* **1965**, *87*, 3695.
(29) Hiatt, R.; Mill, T.; Mayo, F. R. *J. Org. Chem.* **1968**, *33*, 1416.
(30) Hiatt, R.; Mill, T.; Irwin, K. C.; Castleman, J. K. *J. Org. Chem.* **1968**, *33*, 1421.
(31) Hiatt, R.; Mill, T.; Irwin, K. C.; Castleman, J. K. *J. Org. Chem.* **1968**, *33*, 1428.
(32) Hiatt, R.; Irwin, K. C.; Gould, C. W. *J. Org. Chem.* **1968**, *33*, 1430.

according to eq 13. This reaction can also initiate the radical

$$\underset{\mathbf{2}}{(TMP)Fe^{III}OO\text{-}t\text{-}Bu} \rightarrow \underset{\mathbf{4}}{(TMP)Fe^{IV}{=}O} + t\text{-}BuO^{\bullet} \quad (13)$$

chain decomposition of *tert*-butyl hydroperoxide. We have shown earlier that $(TMP)Fe^{IV}{=}O$ (**4**) forms upon warming the peroxo-bridged dimer $(TMP)Fe^{III}OOFe^{III}(TMP)$ via eq 14 and 15.[18]

$$2(TMP)Fe^{II} + O_2 \xrightarrow{-70\ ^\circ C} (TMP)Fe^{III}OOFe^{III}(TMP) \quad (14)$$

$$(TMP)Fe^{III}OOFe^{III}(TMP) \xrightarrow{-30\ ^\circ C} \underset{\mathbf{4}}{2(TMP)Fe^{IV}{=}O} \quad (15)$$

Identical ^1H NMR spectral data for **4** are observed for both routes. The ^1H NMR spectrum of **4** shows very small hyperfine shifts, but it is clear that **4** is a paramagnetic species. During warming of $(TMP)Fe^{III}OO\text{-}t\text{-}Bu$, we have seen no evidence for the formation of the green $(TMP^{\bullet})Fe^{IV}{=}O^{+}$ that would result from heterolytic cleavage of the O–O bond of **2**. The ^1H NMR spectrum of $(TMP^{\bullet})Fe^{IV}{=}O^{+}$ (Table I) is sufficiently distinct that we should have had no difficulty in detecting this intermediate had it formed in this reaction. However, Traylor and Xu have presented evidence to show that $(P^{\bullet})Fe^{IV}{=}O^{+}$ reacts rapidly with *tert*-butyl hydroperoxide,[13] and we have separately confirmed by ^1H NMR observations that $(TMP^{\bullet})Fe^{IV}{=}O^{+}$ is readily destroyed by *tert*-butyl hydroperoxide in dichloromethane at −30 °C. Since, however, we detect no *tert*-butyl hydroperoxide at the stage when we see the formation of $(TMP)Fe^{IV}{=}O$, we believe that homolytic O–O bond cleavage is occurring. Warming of **2** to give **4** has been observed under a variety of conditions, but we believe that it is particularly significant that samples containing **2**, which have been stored for 12 h at −80 °C and then warmed, yield **4** and that no *tert*-butyl hydroperoxide can be detected immediately after we detected the formation of **4**. Nevertheless, the initial presence of *tert*-butyl hydroperoxide in this system and the possibility of a reaction between this hydroperoxide and any $(TMP^{\bullet})Fe^{IV}{=}O^{+}$ that might form do produce some level of ambiguity in interpretation. We are continuing work to prepare **2** or a suitable analogue under conditions where no free hydroperoxide is present.

Addition of *N*-methylimidazole to $(TMP)Fe^{III}OO\text{-}t\text{-}Bu$ at −70 °C produces the six-coordinate $(N\text{-MeIm})(TMP)Fe^{IV}{=}O$, presumably according to eq 16. $(N\text{-MeIm})(TMP)Fe^{IV}{=}O$ has been

$$(TMP)Fe^{III}OO\text{-}t\text{-}Bu + N\text{-MeIm} \rightarrow (N\text{-MeIm})(TMP)Fe^{IV}{=}O + t\text{-}BuO^{\bullet} \quad (16)$$

characterized previously by the addition of *N*-MeIm to $(TMP)Fe^{IV}{=}O$.[18] The reaction of **2** with *N*-MeIm is different from that observed for $(TMP)Fe^{III}OOFe^{III}(TMP)$. With $(TMP)Fe^{III}OOFe^{III}(TMP)$, an Fe–O bond is broken and $(N\text{-MeIm})(TMP)FeO_2$ and $(TMP)Fe^{II}(N\text{-MeIm})_2$ are the products. However, *N*-MeIm does react with $(TPP)Fe^{III}OOFe^{III}(TPP)$ to yield $(N\text{-MeIm})(TPP)Fe^{IV}{=}O$; thus, it promotes homolytic O–O bond cleavage. On the basis of studies of metalloporphyrin-catalyzed olefin epoxidation by alkyl hydroperoxides, Mansuy and coworkers suggested that imidazole dramatically activated the system by promoting heterolytic O–O bond cleavage[33] in part through coordination to the metal. Our observations of homolytic cleavage products (eq 16) suggest that simple coordination is not sufficient to induce heterolytic cleavage. Solvent polarity may play a major role in differentiating our observations in a very nonpolar environment (toluene, where homolytic cleavage is favored) from the more polar solvent mixture (dichloromethane/acetonitrile) used in the studies of Mansuy et al.[33] Also, the ability of the imidazole to function as a hydrogen bond donor and acceptor in interacting with the alkyl peroxide may be significant. *N*-Methylimidazole of course cannot function as a hydrogen bond donor. In peroxidases where compound I is the product of heterolytic cleavage, an elaborate hydrogen bonding network is present at the active site and presumably intimately involved in affecting the O–O bond cleavage.[34]

In summary, evidence for the formation of $PFe^{III}OO\text{-}t\text{-}Bu$ from both Fe(II) and Fe(III) precursors has been obtained from these NMR studies, and the decomposition of $PFe^{III}OO\text{-}t\text{-}Bu$ in a nonpolar environment (toluene) appears to occur by homolysis of the O–O bond. Other studies by Bruice,[8] Marnett,[35] and Mansuy[36] and their co-workers also point to homolytic O–O bond cleavage in the reactions of simple iron porphyrins with hydroperoxides.

Experimental Section

Materials. $(TTP)H_2$[24] and $(TMP)H_2$[25] were prepared by previously reported procedures, and iron was inserted by the standard route. Toluene-d_8 (Aldrich) was deoxygenated by three freeze–pump–thaw cycles and stored over 4-Å sieves in a Vacuum Atmosphere glovebox under purified nitrogen. *tert*-Butyl hydroperoxide in 2,2,4-trimethylpentane was purchased from Aldrich Chemical Co.

Reactions with *t*-BuOOH. In a controlled-atmosphere box, a dioxygen-free, toluene-d_8 solution of the appropriate iron porphyrin (3–5 mmol) was placed in an NMR tube, capped with a rubber septum, and sealed with parafilm. The sample was then removed from the controlled-atmosphere box and cooled to −78 °C in a dry ice/ethanol bath. The *t*-BuOOH solution was added via a microsyringe while the sample was maintained at −78 °C to give *t*-BuOOH concentrations in the range 9–50 mmol. The progress of the reaction was followed by NMR spectroscopy, and after warming the organic products were identified by gas chromatography.

Instrumentation. NMR spectra were recorded at 360 and 300 MHz using a Nicolet NT360 or General Electric QE 300 Fourier transform spectrometer operating in the quadrature mode. For a typical paramagnetic spectrum 500–2000 transients were accumulated over a 40-kHz bandwidth with 16K data points, a 6-μs 90° pulse, and a 50-ms delay time. The signal-to-noise ratio was improved by apodization of the free induction decay, which introduced a negligible 15–30-Hz line broadening. For a typical spectral scan of the diamagnetic region 16 transients were collected with a 2-s delay time. The residual methyl peak of toluene was used as a secondary reference, this being set at 2.09 ppm. Capillary gas chromatograms were collected on a Varian 3700 gas chromatograph employing a 15-m Supelco SPB-5 capillary column and a flame ionization detector. Signal integration employed a Varian 4270 integrator. Electronic spectra were recorded on a Hewlett-Packard 9122 diode array spectrometer.

Acknowledgment. We thank the National Institutes of Health (Grant GM 26226) for support and T. G. Traylor, L. J. Marnett, D. Mansuy, and J. P. Ciccone for stimulating discussions.

(33) Mansuy, D.; Battioni, P.; Renaud, J.-P. *J. Chem. Soc., Chem. Commun.* **1984**, 1255. Battioni, P.; Renaud, J.-P.; Bartoli, J. F.; Reina-Artiles, M.; Fort, M.; Mansuy, D. *J. Am. Chem. Soc.* **1988**, *110*, 8462.

(34) Poulos, T. L.; Kraut, J. *J. Biol. Chem.* **1980**, *255*, 8199. Finzel, B. C.; Poulos, T. L.; Kraut, J. *J. Biol. Chem.* **1984**, *259*, 13027. Thanabal, V.; de Ropp, J. S.; La Mar, G. N. *J. Am. Chem. Soc.* **1988**, *110*, 3027.

(35) Dix, T. Z.; Marnett, L. J. *J. Am. Chem. Soc.* **1983**, *105*, 7001. Labeque, R.; Marnett, L. J. *J. Am. Chem. Soc.* **1987**, *109*, 2828. Marnett, L. J., personal communication.

(36) Mansuy, D.; Bartoli, J. F.; Momenteau, M. *Tetrahedron Lett.* **1982**, *23*, 2781. Mansuy, D., personal communication.